

Quantum Fourier Transform in Oscillating Modes

Qi-Ming Chen,^{1,2} Frank Deppe,^{1,2,3,*} Re-Bing Wu,^{4,5} Luyan Sun,⁶ Yu-xi Liu,^{5,7} Yuki Nojiri,^{1,2} Stefan Pogorzalek,^{1,2} Michael Renger,^{1,2} Matti Partanen,¹ Kirill G. Fedorov,^{1,2} Achim Marx,¹ and Rudolf Gross^{1,2,3,†}

¹Walther-Meißner-Institut, Bayerische Akademie der Wissenschaften, 85748 Garching, Germany

²Physik-Department, Technische Universität München, 85748 Garching, Germany

³Munich Center for Quantum Science and Technology (MCQST), Schellingstr. 4, 80799 Munich, Germany

⁴Department of Automation, Tsinghua University, Beijing 100084, China

⁵Beijing National Research Center for Information Science and Technology, Beijing 100084, China

⁶Center for Quantum Information, Institute for Interdisciplinary Information Sciences, Tsinghua University, Beijing 100084, China

⁷Institute of Microelectronics, Tsinghua University, Beijing 100084, China

(Dated: June 9, 2022)

Quantum Fourier transform (QFT) is a key ingredient of many quantum algorithms. In typical applications such as phase estimation, a considerable number of ancilla qubits and gates are used to form a Hilbert space large enough for high-precision results. Qubit recycling reduces the number of ancilla qubits to one, but it is only applicable to semi-classical QFT and requires repeated measurements and feedforward within the coherence time of the qubits. In this work, we explore a novel approach based on resonators that forms a high-dimensional Hilbert space for the realization of QFT. By employing the perfect state-transfer method, we map an unknown multi-qubit state to a single resonator, and obtain the QFT state in the second oscillator through cross-Kerr interaction and projective measurement. A quantitative analysis shows that our method allows for high-dimensional and fully-quantum QFT employing the state-of-the-art superconducting quantum circuits. This paves the way for implementing various QFT related quantum algorithms.

Introduction.—In order to fully explore the quantum advantage in solving computational problems [1, 2], various quantum algorithms have been proposed during the last decades [3]. Among them, quantum Fourier transform (QFT) attracts a particularly high interest since it is the cornerstone of a considerable number of quantum algorithms. Prominent examples are the phase estimation algorithm, as well as its further applications in order-finding and factorization problems [3]. Similar to the Fourier transform in classical computation, the basic idea of QFT is to transform each orthonormal basis state $|m\rangle$ of a q -dimensional Hilbert space into the state

$$|\mathcal{F}(m)\rangle = \left(\frac{1}{\sqrt{q}} \sum_{n=0}^{q-1} e^{i2\pi mn/q} |n\rangle \langle m| \right) |m\rangle. \quad (1)$$

Here, m , n , and q are integer numbers. Hence, the transform on an arbitrary state reads $\sum_{m=0}^{q-1} c_m |m\rangle \rightarrow \sum_{m=0}^{q-1} c_m |\mathcal{F}(m)\rangle$, where c_m are the normalized amplitudes.

To implement QFT in a quantum circuit, one requires $n = \log_2(q)$ qubits as well as n^2 high-fidelity single or two-qubit gates [3]. Typical applications of QFT, such as Shor's factorization algorithm [4] and the Harrow-Hassidim-Lloyd scheme for solving linear equations [5], require a large number of ancilla qubits in addition to those carrying the actual quantum information. These requirements make a scalable implementation of QFT in present-day noisy intermediate-scale quantum (NISQ) devices very challenging. For this reason, to our knowledge, there have been only small-scale demonstrations of QFT with Hilbert spaces spanned

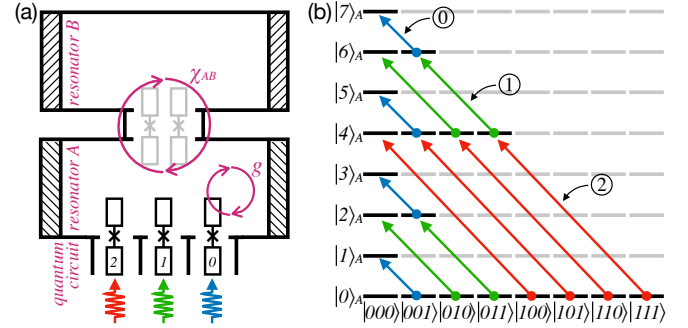


FIG. 1. (a) Physical implementation of the resonator QFT in superconducting quantum circuits, where each qubit in the quantum circuit is coupled to the resonator A through a Jaynes-Cummings interaction with coupling strength g . The two resonators A and B are coupled by a cross-Kerr interaction χ_{AB} , which is realized by mediating a N -type system, for example, two qubits, between the two resonators. Interactions in the system are controlled by the frequencies of the qubits, labelled as 2, 1, 0 for a 3-qubit example, or by engineering the N -type system. (b) State mapping procedure in a 3-qubit example. The horizontal and vertical labels show the multi-qubit state and photon number state in the resonator A, respectively. The red/green/blue-colored arrows, labelled as ②/①/①, respectively, indicate different multi-frequency control fields acting on the 2nd, 1st, and 0th qubit. The excitation of these qubits are transferred into 4, 2, and 1 photons in the resonator A, respectively.

by up to three qubits [6–12]. In certain cases, the number of ancilla qubits can be reduced to one by means of qubit recycling [13–20]. However, n high-precision measurements combined with real-time feedforward are

required within the coherence time of the system. This is technically difficult for large q . More importantly, qubit recycling results in a semi-classical QFT which is not directly applicable to problems where a fully-quantum QFT is required. Here, we propose to use two ancilla harmonic resonators A and B to realize QFT. This approach not only saves qubit resources but also keeps the result fully-quantum, where the coherence in the resulting QFT state is kept and can be further used in quantum information processing. Profiting from the infinite-dimensional Hilbert space of the oscillating mode, one can realize QFT for arbitrary q without scaling up the ancilla system. Figure 1(a) shows a possible implementation of our proposal with superconducting quantum circuits. The protocol consists of three steps: (i) Transfer an arbitrary multi-qubit state from the qubit-based quantum circuit to the resonator A, (ii) Switch on a cross-Kerr interaction between A and B for a suitable time, and (iii) localize the resulting QFT state in B by applying a projective measurement on A. Afterwards, the result can be either transferred back to the quantum circuit for further processing or read out directly from B, depending on the specific applications of QFT.

Transferring a multi-qubit state to the resonator.—To begin our analysis, we first describe the transfer of an unknown n -qubit state to a single resonator, which is also an important problem on its own right. This state can be expressed in a basis, where each basis state is labeled with a binary string indicating the states of the individual qubits. In the string, starting from the right, the k th bit represents a decimal number 2^k . Our goal is to produce a superposition state in the resonator, where each basis state of the n qubits is replaced by a Fock state corresponding to the decimal number of the binary string. For example, in a 3-qubit system the basis state $|110\rangle$ (binary string) is mapped to the Fock state $|6\rangle_A$ (decimal number) in the resonator. The state mapping procedure is then composed of n steps. Specifically, we couple the qubits on resonance with resonator A in *reverse* order, i.e., $k = n - 1, \dots, 0$. For each k , we transfer the population of the states $|m_k, 1\rangle_{A,k}$, where m_k and 1 denote the number of excitations in the resonator A and the k th qubit, to the new state $|m_k + 2^k, 0\rangle_{A,k}$. This is equivalent to the binary-decimal number transform in mathematics, see Fig. 1(b) for a 3-qubit example.

The details of our transfer protocol are described by one of the two following scenarios. For $k > 0$, we adiabatically tune the k th qubit into resonance with the resonator A while keeping the other qubits detuned, such that a suitable Jaynes-Cummings interaction can be generated between the two components. During this process, the initially uncoupled eigenstates $|m_k, 0\rangle_{A,k}$ and $|m_k, 1\rangle_{A,k}$ are transformed into the dressed states $|m_k, -\rangle_{A,k}$ and $|m_k + 1, +\rangle_{A,k}$, respectively, where m_k indicates the photon number in the resonator before coupling to the k th qubit. Here, we define

the eigenstates of the resonant Jaynes-Cummings Hamiltonian as $|0, 0\rangle_{A,k}$ for the ground state and $|m_k, \pm\rangle_{A,k} \equiv (|m_k, 0\rangle_{A,k} \pm |m_k - 1, 1\rangle_{A,k})/\sqrt{2}$ for $m_k > 0$. The corresponding eigenenergies are $E_{m_k, \pm} = \hbar(m_k\omega_A \pm \sqrt{m_k}g)$, where ω_A is the frequency of the resonator A and g is the coupling rate. To transfer the population of this qubit to the resonator, we apply the following multi-frequency control to the qubit

$$V_{\text{map}}^{(k)} = \sum_{m_k} \sum_{l=1}^{2^k-1} (-1)^l \hbar 2\Omega \sqrt{l(2^k-l)} \cos(\omega_{m_k, l} t) \sigma_{x, k}. \quad (2)$$

Here, $\omega_{m_k, l} = (E_{m_k+l+1, +} - E_{m_k+l, -})/\hbar$ for even l and $\omega_{m_k, l} = (E_{m_k+l+1, -} - E_{m_k+l, +})/\hbar$ for odd l , Ω is a scaling factor and $\sigma_{x, k}$ is the standard Pauli operator for the k th qubit. As shown in Fig. 1(b), only resonator states $|m_k\rangle_A$ with $m_k \in \{0, 2^{k+1}, \dots, (2^{n-(k+1)} - 1)2^{k+1}\}$ and $m_k \leq 2^{n-1}$ can have finite occupation before coupling the k th qubit [21]. For each m_k , the control field is equivalent to the one defined in Ref. 22, which couples all the states $|m_k + 1, +\rangle, |m_k + 2, -\rangle, \dots, |m_k + 2^k, -\rangle$ in a chain. Transition from the first to the last states can thus be regarded as transferring a state in a 2^k -long Ising chain, which is in turn equivalent to a rotation of a fictitious spin- $(2^k - 1)/2$ particle [23]. Note that by coupling the qubits in a reverse order, the values of m_k are sufficiently separated from each other. Hence, each driving frequency $\omega_{m_k, l}$ in Eq. (2) is unique and the state transitions for all m_k can happen in parallel. Most importantly, by applying the control field $V_{\text{map}}^{(k)}$ for a time period $\tau_{\text{map}} = \pi/\Omega$, we can realize the transitions $|m_k + 1, +\rangle_{A,k} \rightarrow |m_k + 2^k, -\rangle_{A,k}$ for all m_k within a *single* step. The $|m_k, -\rangle_{A,k}$ states are not influenced because they are not in any of the transition chains. Finally, at the end of each step, we adiabatically detune the k th qubit from the resonator. As a consequence, the dressed states $|m_k, -\rangle_{A,k}$ and $|m_k + 2^k, -\rangle_{A,k}$ are transformed to the uncoupled states $|m_k, 0\rangle_{A,k}$ and $|m_k + 2^k, 0\rangle_{A,k}$. For our 3-qubit example, the coefficient of $|110\rangle$ is mapped to the resonator state via the two steps: $|0\rangle_A |110\rangle \rightarrow |4\rangle_A |010\rangle \rightarrow |6\rangle_A |000\rangle$.

For $k = 0$, the interaction described by Eq. (2) vanishes because the desired transitions are photon number preserving. After adiabatically tuning the 0th qubit into resonance with resonator A, we therefore apply the interaction

$$V_{\text{map}}^{(0)} = \sum_{m_0} \hbar 2\sqrt{2}\Omega (\cos(\omega_+ t) + \cos(\omega_1 t)) \sigma_{x, 0}, \quad (3)$$

to the qubit. Physically, the frequency $\omega_+ = (E_{m_0+2, +} - E_{m_0+1, +})/\hbar$ induces a jump in the Jaynes-Cummings ladder and the frequency $\omega_1 = (E_{m_0+2, +} - E_{m_0+1, -})/\hbar$ corresponds to a qubit rotation. The drive $V_{\text{map}}^{(0)}$ couples the three states $|m_0 + 1, +\rangle_{A,0} \rightarrow |m_0 + 2, +\rangle_{A,0} \rightarrow |m_0 + 1, -\rangle_{A,0}$ in a chain, where the last two states are empty

before applying the driving field. Similar to the $k > 0$ case, we detune the 0th qubit after τ_{map} to implement the transition $|m_0 + 1, -\rangle_{A,0} \rightarrow |m_0 + 1, 0\rangle_{A,0}$. Then, all the qubits are off-resonant to the resonator A, inhibiting any further qubit-resonator interactions. All in all, the n -qubit state is successfully transferred to the resonator A by n steps, while the qubits are automatically reset to the ground state.

The performance of our protocol can be benchmarked using the experimentally achievable parameters in typical superconducting quantum circuits. We choose $\Omega/2\pi \simeq 5$ MHz and estimate the total driving time as $n \times 100$ ns for an arbitrary n -qubit quantum state transfer. On the other hand, considering a qubit anharmonicity $\alpha/2\pi \simeq -200$ MHz and a coupling strength $g/2\pi \simeq 200$ MHz, the adiabatic frequency tuning requires $\tau_{\text{ad}} \simeq 100$ ns to fulfill the adiabatic condition $1/\tau_{\text{ad}} \ll |g|, |\alpha|$. In total, we estimate the time required for a n -qubit state transfer to $\tau_1 \simeq n \times 300$ ns. Hence, with the state-of-the-art coherence times of qubits exceeding $50 \mu\text{s}$ [24] and single-photon lifetimes in 3D microwave resonators up to around 10 ms [25], we estimate that a 10-qubit state mapping could be achievable in current experiments, which requires qubit and single-photon lifetimes larger than $3 \mu\text{s}$ and 3 ms, respectively.

Implementing QFT in two coupled resonators.—After having discussed the mapping of the qubit state onto the resonator A, we describe the coupling of a second resonator B to resonator A by the cross-Kerr interaction

$$V_{\text{Kerr}} = \hbar\chi_{AB}a^\dagger ab^\dagger b, \quad (4)$$

where χ_{AB} is the coupling strength between the two resonators. In superconducting quantum circuits, a cross-Kerr interaction with strength $\chi_{AB}/2\pi \simeq 2.5$ MHz has been reported by coupling N -type system to both resonators, e.g., two qubits as shown in Fig. 1(a) [26, 27]. However, as will be discussed later, a weak cross-Kerr interaction around several kilohertz is already sufficient for implementing QFT in our protocol.

Upon transfer of an n -qubit state using the method described above, the state of resonator A is

$$|\psi(\tau_1)\rangle_A = \sum_{m=0}^{q-1} c_m |m\rangle_A. \quad (5)$$

Furthermore, we assume that the resonator B is prepared in the state

$$|\psi(\tau_1)\rangle_B = \frac{1}{\sqrt{q}}(|0\rangle_B + |1\rangle_B + \dots + |q-1\rangle_B), \quad (6)$$

which can be realized by employing one of the methods studied in Refs. 28–31. Then, the free evolution of the two-mode system under the cross-Kerr interaction of Eq. (4) reads

$$|\psi(\tau_1 + t)\rangle_{AB} = \sum_{m=0}^{q-1} c_m |m\rangle_A \frac{1}{\sqrt{q}} \sum_{n=0}^{q-1} e^{-i\chi_{AB}tmn} |n\rangle_B. \quad (7)$$

After waiting for a time period $\tau_2 = (-2\pi/q + 2k\pi)/\chi_{AB}$ with k being an arbitrary integer such that $\tau_2 > 0$, we obtain the state

$$|\psi(\tau_1 + \tau_2)\rangle_{AB} = \sum_{m=0}^{q-1} c_m |m\rangle_A |\mathcal{F}(m)\rangle_B. \quad (8)$$

Then, we control the N -type system between the two resonators to suppress the cross-Kerr interaction as described in Refs. 26 and 27. For each m , one can immediately see that the states in resonator B correspond to the Fourier transform of the basis states $|m\rangle_A$ as defined in Eq. (1). Similarly, the inverse quantum Fourier transform (QFT $^{-1}$) can be realized by following the same process but setting $\tau_2 = (+2\pi/q + 2k\pi)/\chi_{AB}$.

If we assume $\chi_{AB}/2\pi = \pm 50$ kHz with the sign controlled by the N -type system, the QFT or QFT $^{-1}$ processes require a time duration of $\tau_2 \simeq (20/q) \mu\text{s}$. Considering the dissipation of the resonator, i.e., the $1/m$ dependence for the lifetime of the m -photon Fock state, our method requires a single-photon lifetime larger than $20 \mu\text{s}$, independent of the dimension of the Hilbert space q . Taking into account the higher-order nonlinearities that may exist in the resonator and the potential use of optimal control methods, we expect the required single-photon lifetime not to exceed $\sim 100 \mu\text{s}$ [32, 33]. Note that this value is still one order of magnitude smaller than the value of about 3 ms estimated above for the transfer of a 10-qubit state. Hence, we conclude that it is the state transfer process that limits the achievable dimension q . This indicates that only a relatively weak cross-Kerr interaction is required in the system, which leaves substantial freedom in the sample fabrication and the required responding speed of the instruments.

Projective measurement on the resonator.—To further extract the QFT state from the two resonators, one needs to disentangle the two resonators while keeping the coherence among different $|\mathcal{F}(m)\rangle_B$. In our design, we project the resonator A onto the state $|p\rangle_A = \sum_{m=0}^{q-1} |m\rangle_A / \sqrt{q}$, which is realized by the following two steps. In the first step, we reverse the state transfer method introduced above to transfer the entanglement between the resonators A and B to that between the n qubits in the quantum circuit and resonator B. This procedure requires a time duration of τ_1 . Next, we apply n projective measurements along the X-direction for each qubit, which effectively realizes the projection $|p\rangle\langle p|$ on the n qubits. The detection of the qubits in state $|p\rangle$ results in the following state of the whole system

$$|\psi(2\tau_1 + \tau_2 + \tau_3)\rangle = |0\rangle_A \otimes \left(\sum_{m=0}^{q-1} c_m |\mathcal{F}(m)\rangle_B \right) \otimes |p\rangle, \quad (9)$$

where τ_3 indicates the time duration for n projective measurements on the qubits. In this way, the QFT state is entirely localized in resonator B. The success

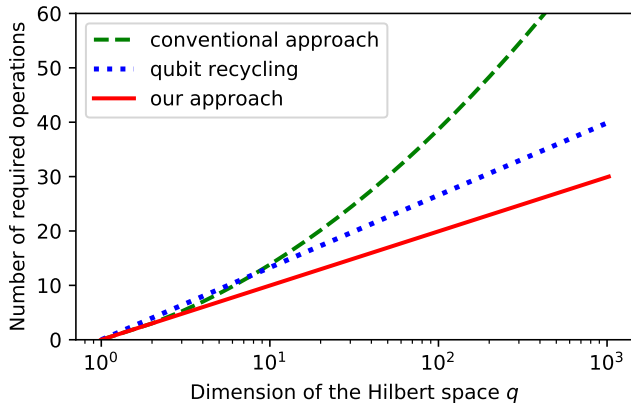


FIG. 2. Comparison of the required number of operations within the coherence time of the system for realizing a q -dimensional quantum phase estimation. Here, we assume the projective measurement in our approach is successful, which is confirmed by data post-selection. The number of controlled-U gates is the same for the three approaches and is not counted in this comparison. The circuit diagrams for the three approaches and a detailed derivation of these numbers can be found in the supplemental material [21].

probability of the detection result $|p\rangle$ is $P = 1/q$, which is independent of the specific state in the two resonators.

For large q , this small probability implies a considerable number of repeated measurements. In each repeat, we reset the qubits and resonators, do state transfer, free evolution, and a set of projective measurements on qubits. Then, post-selection is needed to distinguish the successful measurements from the data. However, we note that the number of repeated measurements is not limited by the decoherence time of the system. Our method provides a possible way to realize high-dimensional and fully-quantum QFT at the price of a large number of repeated measurements, which is otherwise hardly achievable by using the existing methods because of the currently limited qubit lifetime.

Realizing high-precision quantum phase estimation.— In order to illustrate a possible application of our QFT method, we discuss how to realize high-precision quantum phase estimation with one ancilla qubit and two resonators. Assuming that the unitary operator U acting on the multi-qubit state $|\psi\rangle$ results in an unknown phase θ , i.e., $U|\psi\rangle = e^{i\theta}|\psi\rangle$, the aim of quantum phase estimation is to determine θ by using QFT^{-1} . To transfer the phase information from the quantum circuit to a single resonator, we build a sequence of controlled-U gates between the ancilla qubit and the quantum circuit [21]. Before every controlled-U gate, the ancilla qubit is prepared in $|\psi\rangle_a = \frac{1}{\sqrt{2}}(|0\rangle_a + |1\rangle_a)$ by a Hadamard gate. After each controlled-U gate, we employ the state mapping method and implement the following transition $|1\rangle_a \otimes |m\rangle_A \rightarrow |0\rangle_a \otimes |m + 2^k\rangle_A$. This state mapping

process also resets the ancilla qubit to the ground state, so that it can be recycled straightforwardly. After n steps, we obtain the following state in the resonator A

$$|\psi(\tau_1)\rangle_A = \frac{1}{\sqrt{q}} \sum_{m=0}^{q-1} e^{im\theta} |m\rangle_A. \quad (10)$$

Next, we couple the resonator B to A through a cross-Kerr interaction and implement QFT^{-1} in the oscillating modes. As discussed before, the free evolution for a time period τ_2 takes the system to the following state

$$|\psi(\tau_1 + \tau_2)\rangle_{AB} = \frac{1}{q} \sum_{m=0}^{q-1} |m\rangle_A \sum_{n=0}^{q-1} e^{im(\theta - 2\pi n/q)} |n\rangle_B. \quad (11)$$

Finally, we perform a projective measurement on the resonator A to disentangle the two resonators and obtain the following state in B

$$|\psi(2\tau_1 + \tau_2 + \tau_3)\rangle_B \approx |[q\theta/2\pi]\rangle_B, \quad (12)$$

where $[q\theta/2\pi]$ represents the nearest integer to $q\theta/2\pi$. We note that this approximation becomes an equality when $q\theta/2\pi$ is an integer. This observation indicates that the phase θ can be estimated by measuring the photon number in resonator B. The estimation precision is $\pm\pi/q$, which is proportional to the inverse of the Hilbert space dimension q .

In FIG. 2 we compare the number of operations required within the coherence time of the system for realizing a q -dimensional quantum phase estimation in the conventional approach, qubit recycling, and our approach. We note that because of the non-unitary success probability of our approach, one may reset and repeat the whole process several times and use post-selection to distinguish the successful measurements. However, this repeat number is not limited by the coherence time, such that it is not counted in the comparison. The resources are then: (i) conventional approach: $n = \log_2(q)$ ancilla qubits and $2n + n(n+1)/2$ operations, (ii) qubit recycling: 1 ancilla qubit and $4n$ operations, and (iii) our approach: 1 ancilla qubit and 2 resonators, and $3n$ operations [21]. We see that both (ii) and (iii) reduce the qubit resources and the number of operations to a large extent, as compared to (i). However, qubit recycling, (ii), requires n real-time measurements and measurement-based single-qubit gates within the coherence time of the quantum circuit, which is a significant challenge considering current fabrication, measurement, and control technologies. More importantly, it is indeed a semi-classical QFT method which cannot be directly used in the quantum algorithms where fully-quantum QFT is desired, e.g., for solving linear equations [5, 10]. The above observations reveal that our method, (iii), not only saves hardware resources such as ancilla qubits and gates, but also

realizes full-quantum QFT which is desired in many quantum algorithms.

Conclusions and outlook.—In this work, we propose to use two harmonic resonators with a tunable cross-Kerr interaction to realize QFT in a superconducting quantum circuit architecture. The harmonic resonator has the advantage of a large dimension of the Hilbert space and a long coherence time. In this way, it is possible to implement complex operations regardless of the depth of the quantum circuit and the relatively short qubit coherence time. The whole procedure consists of the transfer of the multi-qubit state to a single resonator, the free evolution in two coupled resonators, and the projective measurement in one resonator. It avoids the need for a large number of qubits, gates, and measurements as required in conventional QFT related quantum algorithms, and realizes fully-quantum QFT in contrast to qubit recycling. A quantitative analysis shows that a 2^{10} -dimensional QFT can be realized in the state-of-the-art superconducting quantum circuits, which is large enough for most applications in quantum computation. Moreover, our study reveals that the harmonic resonators can be very useful in qubit-based quantum circuits, which may work as an ancilla system to implement otherwise rather difficult quantum operations, such as QFT. This combination provides the possibility of realizing various kinds of quantum algorithms in the NISQ devices.

The authors note that the estimate made for a 2^{10} -dimensional QFT in this study is mainly determined by the state-transfer process, given the control parameters we choose and the 10ms single-photon lifetime of the microwave resonator reported in the literature. However, the qubit lifetime is not a major concern, since only several microseconds are needed in our protocol. To accommodate more qubits, one needs either a longer resonator lifetime or a shorter state-transfer time. Whereas the former is beyond the scope of this discussion, the latter may be achieved by optimizing the circuit parameters or using the short-time techniques within the adiabatic frequency tuning process, such as the counter-diabatic pulses [34].

Acknowledgements.—We acknowledge support by the German Research Foundation via Germany’s Excellence Strategy EXC-2111-390814868, the Elite Network of Bavaria through the program ExQM, the European Union via the Quantum Flagship project QMiCS (Grant No.820505). R.B.W. acknowledges supports from the National Key Research and Development Program of China through Grant No.2017YFA0304304, and NSFC Grants No.61773232 and No.61833010. L.S. acknowledges the support from National Key Research and Development Program of China Grant No.2017YFA0304303 and National Natural Science Foundation of China Grant No.11474177. Y.X.L. is supported by Key-Area Research and Development

Program of GuangDong Province under Grant No.2018B030326001.

* frank.deppe@wmi.badw.de

† rudolf.gross@wmi.badw.de

- [1] C. Neill, P. Roushan, K. Kechedzhi, S. Boixo, S. V. Isakov, V. Smelyanskiy, A. Megrant, B. Chiaro, A. Dunsworth, K. Arya, R. Barends, B. Burkett, Y. Chen, Z. Chen, A. Fowler, B. Foxen, M. Giustina, R. Graff, E. Jeffrey, T. Huang, J. Kelly, P. Klimov, E. Lucero, J. Mutus, M. Neeley, C. Quintana, D. Sank, A. Vainsencher, J. Wenner, T. C. White, H. Neven, and J. M. Martinis, *Science* **360**, 195 (2018).
- [2] F. Arute, K. Arya, R. Babbush, D. Bacon, J. C. Bardin, R. Barends, R. Biswas, S. Boixo, F. G. S. L. Brandao, D. A. Buell, B. Burkett, Y. Chen, Z. Chen, B. Chiaro, R. Collins, W. Courtney, A. Dunsworth, E. Farhi, B. Foxen, A. Fowler, C. Gidney, M. Giustina, R. Graff, K. Guerin, S. Habegger, M. P. Harrigan, M. J. Hartmann, A. Ho, M. Hoffmann, T. Huang, T. S. Humble, S. V. Isakov, E. Jeffrey, Z. Jiang, D. Kafri, K. Kechedzhi, J. Kelly, P. V. Klimov, S. Knysh, A. Korotkov, F. Kostritsa, D. Landhuis, M. Lindmark, E. Lucero, D. Lyakh, S. Mandr, J. R. McClean, M. McEwen, A. Megrant, X. Mi, K. Michielsen, M. Mohseni, J. Mutus, O. Naaman, M. Neeley, C. Neill, M. Y. Niu, E. Ostby, A. Petukhov, J. C. Platt, C. Quintana, E. G. Rieffel, P. Roushan, N. C. Rubin, D. Sank, K. J. Satzinger, V. Smelyanskiy, K. J. Sung, M. D. Trevithick, A. Vainsencher, B. Villalonga, T. White, Z. J. Yao, P. Yeh, A. Zalcman, H. Neven, and J. M. Martinis, *Nature* **574**, 505 (2019).
- [3] M. A. Nielsen and I. L. Chuang, *Quantum Computation and Quantum Information* (Cambridge University Press, 2010).
- [4] P. W. Shor, in *Proceedings 35th Annual Symposium on Foundations of Computer Science* (1994) pp. 124–134; P. W. Shor, *SIAM Rev.* **41**, 303 (1999).
- [5] A. W. Harrow, A. Hassidim, and S. Lloyd, *Phys. Rev. Lett.* **103**, 150502 (2009).
- [6] Y. S. Weinstein, M. A. Pravia, E. M. Fortunato, S. Lloyd, and D. G. Cory, *Phys. Rev. Lett.* **86**, 1889 (2001).
- [7] L. M. K. Vandersypen, M. Steffen, G. Breyta, C. S. Yannoni, M. H. Sherwood, and I. L. Chuang, *Nature* **414**, 883 (2001).
- [8] A. Politi, J. C. F. Matthews, and J. L. O’Brien, *Science* **325**, 1221 (2009).
- [9] E. Lucero, R. Barends, Y. Chen, J. Kelly, M. Mariantoni, A. Megrant, P. OMalley, D. Sank, A. Vainsencher, J. Wenner, T. White, Y. Yin, A. N. Cleland, and J. M. Martinis, *Nat. Phys.* **8**, 719 (2012).
- [10] X. D. Cai, C. Weedbrook, Z. E. Su, M. C. Chen, M. Gu, M. J. Zhu, L. Li, N. L. Liu, C. Y. Lu, and J. W. Pan, *Phys. Rev. Lett.* **110**, 230501 (2013).
- [11] J. Pan, Y. Cao, X. Yao, Z. Li, C. Ju, H. Chen, X. Peng, S. Kais, and J. Du, *Phys. Rev. A* **89**, 022313 (2014).
- [12] Y. Zheng, C. Song, M.-C. Chen, B. Xia, W. Liu, Q. Guo, L. Zhang, D. Xu, H. Deng, K. Huang, Y. Wu, Z. Yan, D. Zheng, L. Lu, J.-W. Pan, H. Wang, C.-Y. Lu, and X. Zhu, *Phys. Rev. Lett.* **118**, 210504 (2017).

- [13] R. B. Griffiths and C. S. Niu, *Phys. Rev. Lett.* **76**, 3228 (1996).
- [14] S. Parker and M. B. Plenio, *Phys. Rev. Lett.* **85**, 3049 (2000).
- [15] C. Y. Lu, D. E. Browne, T. Yang, and J. W. Pan, *Phys. Rev. Lett.* **99**, 250504 (2007).
- [16] B. P. Lanyon, T. J. Weinhold, N. K. Langford, M. Barbieri, D. F. V. James, A. Gilchrist, and A. G. White, *Phys. Rev. Lett.* **99**, 250505 (2007).
- [17] E. Martin-Lopez, A. Laing, T. Lawson, R. Alvarez, X. Q. Zhou, and J. L. O'Brien, *Nat. Photon.* **6**, 773 (2012).
- [18] X. Q. Zhou, P. Kalasuwan, T. C. Ralph, and J. L. O'Brien, *Nat. Photon.* **7**, 223 (2013).
- [19] J. A. Smolin, G. Smith, and A. Vargo, *Nature* **499**, 163 (2013).
- [20] T. Monz, D. Nigg, E. A. Martinez, M. F. Brandl, P. Schindler, R. Rines, S. X. Wang, I. L. Chuang, and R. Blatt, *Science* **351**, 1068 (2016).
- [21] See Supplementary Materials for additional details.
- [22] F. W. Strauch, *Phys. Rev. Lett.* **109**, 210501 (2012).
- [23] M. Christandl, N. Datta, A. Ekert, and A. J. Landahl, *Phys. Rev. Lett.* **92**, 187902 (2004); M. Christandl, N. Datta, T. C. Dorlas, A. Ekert, A. Kay, and A. J. Landahl, *Phys. Rev. A* **71**, 032312 (2005).
- [24] C. Axline, M. Reagor, R. Heeres, P. Reinhold, C. Wang, K. Shain, W. Pfaff, Y. Chu, L. Frunzio, and R. J. Schoelkopf, *Appl. Phys. Lett.* **109**, 042601 (2016).
- [25] M. Reagor, H. Paik, G. Catelani, L. Sun, C. Axline, E. Holland, I. M. Pop, N. A. Masluk, T. Brecht, L. Frunzio, M. H. Devoret, L. Glazman, and R. J. Schoelkopf, *Appl. Phys. Lett.* **102**, 192604 (2013); M. Reagor, W. Pfaff, C. Axline, R. W. Heeres, N. Ofek, K. Sliwa, E. Holland, C. Wang, J. Blumoff, K. Chou, M. J. Hatridge, L. Frunzio, M. H. Devoret, L. Jiang, and R. J. Schoelkopf, *Phys. Rev. B* **94**, 014506 (2016).
- [26] S. Rebić, J. Twamley, and G. J. Milburn, *Phys. Rev. Lett.* **103**, 150503 (2009).
- [27] Y. Hu, G. Q. Ge, S. Chen, X. F. Yang, and Y. L. Chen, *Phys. Rev. A* **84**, 012329 (2011).
- [28] Y. X. Liu, L. F. Wei, and F. Nori, *Europhys. Lett.* **67**, 941 (2004).
- [29] M. Hofheinz, E. Weig, M. Ansmann, R. C. Bialczak, E. Lucero, M. Neeley, O. AD, H. Wang, J. M. Martinis, and A. Cleland, *Nature* **454**, 310 (2008); M. Hofheinz, H. Wang, M. Ansmann, R. C. Bialczak, E. Lucero, M. Neeley, O. AD, D. Sank, J. Wenner, J. M. Martinis, and A. Cleland, *Nature* **459**, 546 (2009).
- [30] F. W. Strauch, K. Jacobs, and R. W. Simmonds, *Phys. Rev. Lett.* **105**, 050501 (2010); F. W. Strauch, D. Onyango, K. Jacobs, and R. W. Simmonds, *Phys. Rev. A* **85**, 022335 (2012); R. Sharma and F. W. Strauch, *Phys. Rev. A* **93**, 012342 (2016).
- [31] W. Wang, L. Hu, Y. Xu, K. Liu, Y. Ma, S. B. Zheng, R. Vijay, Y. P. Song, L. M. Duan, and L. Sun, *Phys. Rev. Lett.* **118**, 223604 (2017).
- [32] W. S. Warren, H. Rabitz, and M. Dahleh, *Science* **259**, 1581 (1993); H. Rabitz, R. de Vivie-Riedle, M. Motzkus, and K. Kompa, *Science* **288**, 824 (2000).
- [33] R. W. Heeres, P. Reinhold, N. Ofek, L. Frunzio, L. Jiang, M. H. Devoret, and R. J. Schoelkopf, *Nat. Commun.* **8**, 94 (2017).
- [34] A. del Campo, *Phys. Rev. Lett.* **111**, 100502 (2013).

Supplementary Materials for "Quantum Fourier Transform in Oscillating Modes"

Qi-Ming Chen,^{1,2} Frank Deppe,^{1,2,3,*} Re-Bing Wu,^{4,5} Luyan Sun,⁶ Yu-xi Liu,^{5,7} Yuki Nojiri,^{1,2} Stefan Pogorzalek,^{1,2} Michael Renger,^{1,2} Matti Partanen,¹ Kirill G. Fedorov,^{1,2} Achim Marx,¹ and Rudolf Gross^{1,2,3,†}

¹Walther-Meißner-Institut, Bayerische Akademie der Wissenschaften, 85748 Garching, Germany

²Physik-Department, Technische Universität München, 85748 Garching, Germany

³Munich Center for Quantum Science and Technology (MCQST), Schellingstr. 4, 80799 Munich, Germany

⁴Department of Automation, Tsinghua University, Beijing 100084, China

⁵Beijing National Research Center for Information Science and Technology, Beijing 100084, China

⁶Center for Quantum Information, Institute for Interdisciplinary Information Sciences, Tsinghua University, Beijing 100084, China

⁷Institute of Microelectronics, Tsinghua University, Beijing 100084, China

(Dated: June 9, 2022)

I. THE MODEL

As it is schematically shown in the Fig. 1(a) in the main text, we consider a system with n superconducting qubits as well as two microwave resonators coupled by a cross-Kerr interaction. The total Hamiltonian of such a system $H_S = H_0 + V$ can be written as

$$H_0 = \hbar\omega_A a^\dagger a + \hbar\omega_B b^\dagger b + \frac{1}{2} \sum_{k=0}^{n-1} \hbar\omega_k \sigma_{z,k}, \quad (\text{S.1})$$

$$V = \sum_{k=0}^{n-1} \hbar g_k (a^\dagger \sigma_{-,k} + a \sigma_{+,k}) + \hbar \chi_{AB} a^\dagger a b^\dagger b \quad (\text{S.2})$$

Here, ω_A (ω_B), a (b), and a^\dagger (b^\dagger) are the resonance frequency, annihilation, and creation operators of the oscillating mode in resonator A (B), respectively. The symbols ω_k , $\sigma_{z,k}$, $\sigma_{\pm,k}$ are the frequency and standard Pauli operators for the k th qubit in the ensemble. Furthermore, g_k is the coupling rate between resonator A and the k th qubit and χ_{AB} is the cross-Kerr interacting rate between the two resonators. We note that g_k can be neglected in the rotating-wave approximation if the resonator A and the k th qubit are far detuned. The Kerr interaction can be turned on and off by controlling the N -type system coupled between the two resonators, with the method shown in Refs. 1, 2. Throughout this study, we use the interaction picture where $H_I = e^{\frac{i}{\hbar} H_0 t} V e^{-\frac{i}{\hbar} H_0 t}$.

II. TRANSFORMING THE k th QUBIT EXCITATION INTO 2^k PHOTONS IN THE RESONATOR

The method of transferring an n -qubit state to the resonator A consists of n steps. Here, we discuss the $(n - k)$ th step where the excitation of the k th qubit is transformed into 2^k photons in the resonator. Let us suppose that the initial state of the k th qubit is $c_0|0\rangle_k + c_1|1\rangle_k$, where c_0 and c_1 are normalized amplitudes. By adiabatically tuning the qubit and the resonator on resonance, the total state of the combined system reads

$$|\psi(0)\rangle_{A,k} = \sum_m (c_0|m, -\rangle_{A,k} + c_1|m + 1, +\rangle_{A,k}), \quad (\text{S.3})$$

where $m = 0, 2^{k+1}, \dots, (n - 1 - k)2^{k+1}$ represents all the possible photon numbers that are already present in the resonator A before coupling the k th qubit. To proceed, we define the eigenenergies and eigenstates of the on-resonant Jaynes-Cummings Hamiltonian as

$$E_{m,\pm} = \hbar(m\omega_a \pm \sqrt{mg}), \quad |m, \pm\rangle_{A,k} = \frac{1}{\sqrt{2}} (|m, 0\rangle_{A,k} \pm |m - 1, 1\rangle_{A,k}), \quad (\text{S.4})$$

where m and the number 0/1 represent the excitation number in the resonator A and the k th qubit, respectively, and $g = g_k$ for the simplicity of notation.

As illustrated in the main text, for $k \neq 0$ we apply the following control field to the system

$$V_{\text{map}}^{(k)} = \sum_m \sum_{l=1}^{2^k-1} (-1)^l \hbar 2\Omega \sqrt{l(2^k - l)} \cos(\omega_l t) \sigma_{x,k}, \quad (\text{S.5})$$

with $\omega_l = E_{m+l+1,+} - E_{m+l,-}$ for l being *even* or $\omega_l = E_{m+l+1,-} - E_{m+l,+}$ for l being *odd*. Here, Ω relates to the driving amplitude and the above interaction can be regarded as a generalization of the so called ‘‘all-resonant’’ control method [3]. In the interaction picture, the effective Hamiltonian reads

$$H_I = \hbar f(t) \sum_{j \neq k} A,k \langle j | \sigma_{x,k} | k \rangle_{A,k} e^{\frac{i}{\hbar}(E_j - E_k)t} | j \rangle_{A,k} \langle k |, \quad (\text{S.6})$$

where $|j\rangle_{A,k}$ represents the eigenstate corresponding to the eigenvalue E_j for the system. Using the rotating-wave approximation, we find that the only non-zero elements of the effective Hamiltonian are

$$A,k \langle m+l+1, \pm | H_I | m+l, \mp \rangle_{A,k} = \hbar \frac{\Omega}{2} \sqrt{l(2^k - l)}. \quad (\text{S.7})$$

This observation indicates that the driving field couples the states $|m+l, -\rangle_{A,k}$, $|m+l+1, +\rangle_{A,k}$, $|m+l+2, -\rangle_{A,k}$, \dots in a one-dimensional chain, and according to the results in perfect state transfer, the initial state $|m+1, +\rangle$ will be transferred to the final state $|m+2^k, -\rangle$ after time $\tau_{\text{map}} = \pi/\Omega$ [4]. The initial state $|m, -\rangle$ will stay invariant since it is not coupled to any other states in the effective Hamiltonian. In total, the system evolves to the following state after time τ_{map}

$$|\psi(\tau_{\text{map}})\rangle_{A,k} = \sum_m (c_0 |m, -\rangle_{A,k} + c_1 |m+2^k, -\rangle_{A,k}). \quad (\text{S.8})$$

Then, we adiabatically decouple the k th qubit and the resonator A and obtain

$$|\psi(\tau_{\text{map}})\rangle_{A,k} = \sum_m (c_0 |m\rangle_A + c_1 |m+2^k\rangle_A) |0\rangle_k, \quad (\text{S.9})$$

which means that the excitation of the k th qubit is transformed into additional 2^k photons in the resonator A.

III. EXAMPLE: TRANSFERRING A THREE-QUBIT STATE TO A SINGLE RESONATOR

In this section, we discuss how to transfer a 3-qubit state to a single resonator as an example. In a similar fashion, one can extend the results to an arbitrary n -qubit state transfer problem. We write the state of the three qubits as

$$|\psi(0)\rangle = \sum_{m=0}^7 c_m |m\rangle, \quad (\text{S.10})$$

where m can be either in decimal or in binary units. For example, we can write $|5\rangle = |101\rangle$, where we denote the rightmost bit as the 0th qubit and the first as the 2nd qubit. To transfer $|\psi\rangle$ to resonator A, we repeat the method introduced in Sec. II twice, which is followed by an additional photon preserving control.

In the first step, we consider the subsystem composed of the 2nd qubit and the resonator. The initial state of the whole system can be written as

$$|\psi(0)\rangle = |1, +\rangle_{A,2} (c_7 |3\rangle_{1,0} + c_6 |2\rangle_{1,0} + c_5 |1\rangle_{1,0} + c_4 |0\rangle_{1,0}) + |0, -\rangle_{A,2} (c_3 |3\rangle_{1,0} + c_2 |2\rangle_{1,0} + c_1 |1\rangle_{1,0} + c_0 |0\rangle_{1,0}), \quad (\text{S.11})$$

where $|0\rangle_{1,0} = |00\rangle$, $|1\rangle_{1,0} = |01\rangle$, $|2\rangle_{1,0} = |10\rangle$, $|3\rangle_{1,0} = |11\rangle$ are the states for the 1st and the 0th qubits. The subscript indicates the corresponding qubit(s) number. By adiabatically tuning the 2nd qubit into resonance with the resonator, while leaving the other qubits far detuned, the subsystem can be described by the on-resonant Jaynes-Cummings model. Then, we apply the multi-frequency control pulses introduced in Sec. II to transfer $|1, +\rangle_{A,2}$ to $|4, -\rangle_{A,2}$ while leaving $|0, -\rangle_{A,2}$ unchanged. Next, we adiabatically detune them in a way that the dressed states $|4, -\rangle_{A,2}$ and $|0, -\rangle_{A,2}$ become $|4\rangle_A |0\rangle_2$ and $|0\rangle_A |0\rangle_2$, respectively. The state of the whole system thus reads

$$|\psi(\tau_{\text{map}})\rangle = [|4\rangle_A (c_7 |3\rangle_{1,0} + c_6 |2\rangle_{1,0} + c_5 |1\rangle_{1,0} + c_4 |0\rangle_{1,0}) + |0\rangle_A (c_3 |3\rangle_{1,0} + c_2 |2\rangle_{1,0} + c_1 |1\rangle_{1,0} + c_0 |0\rangle_{1,0})] |0\rangle_2. \quad (\text{S.12})$$

In the second step, we adiabatically tune the 1st qubit into resonance with the resonator. The system becomes

$$\begin{aligned} |\psi(\tau_{\text{map}})\rangle = & [|5, +\rangle_{A,1} (c_7 |1\rangle_0 + c_6 |0\rangle_0) + |4, -\rangle_{A,1} (c_5 |1\rangle_0 + c_4 |0\rangle_0) + |1, +\rangle_{A,1} (c_3 |1\rangle_0 + c_2 |0\rangle_0) \\ & + |0, -\rangle_{A,1} (c_1 |1\rangle_0 + c_0 |0\rangle_0)] |0\rangle_2. \end{aligned} \quad (\text{S.13})$$

By using the same method, we realize the state transition $|5, +\rangle_{A,1} \rightarrow |6, -\rangle_{A,1}$ and $|1, +\rangle_{A,1} \rightarrow |2, -\rangle_{A,1}$. After the adiabatic detuning procedure, we obtain

$$|\psi(2\tau_{\text{map}})\rangle = [|6\rangle_A (c_7|1\rangle_0 + c_6|0\rangle_0) + |4\rangle_A (c_5|1\rangle_0 + c_4|0\rangle_0) + |2\rangle_A (c_3|1\rangle_0 + c_2|0\rangle_0) + |0\rangle_A (c_1|1\rangle_0 + c_0|0\rangle_0)]|0\rangle_{2,1}. \quad (\text{S.14})$$

In the last step, we wish to transform the excitation of the 0th qubit to a single extra photon in the resonator A, which is photon preserving and not achievable by using the ‘‘all-resonant’’ control method. However, the basic idea remains that one should construct 2^{n-1} parallel interaction chains between the initial and the final state, and use the perfect state transfer condition to determine the optimal coupling strength between each pair of nodes. One can verify that the multi-frequency control field described by Eq. (3) in the main text couples the three states $|m_0 + 1, +\rangle_{A,0} \rightarrow |m_0 + 2, +\rangle_{A,0} \rightarrow |m_0 + 1, -\rangle_{A,0}$ in a perfect state transfer chain, where the last two states are empty before applying the field. Thus, by adiabatically tuning the resonator A and the 0th qubit into resonance and applying the above field to the 0th qubit, we realize the state transition $|m_0 + 1, +\rangle_{A,0} \rightarrow |m_0 + 1, -\rangle_{A,0}$. Here, $m_0 = 0, 2, 4, 6$ is the possible photon numbers in the resonator that is the result of the first two steps. The final state after the adiabatic detuning is

$$|\psi(3\tau_{\text{map}})\rangle = \left(\sum_{m=0}^7 c_m |m\rangle_A \right) |0\rangle_{2,1,0}. \quad (\text{S.15})$$

By comparing with the initial 3-qubit state shown in Eq. (S.10), we see that an arbitrary 3-qubit state is perfectly transferred to the resonator after 3 steps.

CIRCUIT DIAGRAMS FOR QUANTUM PHASE ESTIMATION

Figure 1 compares the circuit diagrams for (a) the conventional approach, (b) qubit recycling, and (c) our approach in quantum phase estimation. For a Hilbert space with dimension $q = 2^n$, the three approaches require n ancilla qubits, 1 ancilla qubit, and 1 ancilla qubit and 2 resonators, respectively. Within the coherence time of the whole system, the conventional approach requires n Hadamard gates, $n(n+1)/2$ single or two-qubit gates for QFT⁻¹ and n measurements. Qubit recycling requires n Hadamard gates, n real-time measurements, n measurement-based single qubit gates, and n qubit resetting gates. Our approach requires $2n$ times of single-qubit state transfer, and n measurements. The number of controlled-U gates is n , which is the same for the three approaches. We also note that the success probability in our approach is not unitary, which indicates that it should be repeated several times and the data post-selection is required to distinguish the successful measurements from the data. However, as is discussed in the main text, this number of repeated measurements is not limited by the coherence time of the system.

* Electronic address: frank.deppe@wmi.badw.de

† Electronic address: rudolf.gross@wmi.badw.de

- [1] S. Rebić, J. Twamley, and G. J. Milburn, Phys. Rev. Lett. **103**, 150503 (2009), URL <https://link.aps.org/doi/10.1103/PhysRevLett.103.150503>.
- [2] Y. Hu, G. Q. Ge, S. Chen, X. F. Yang, and Y. L. Chen, Phys. Rev. A **84**, 012329 (2011), URL <https://link.aps.org/doi/10.1103/PhysRevA.84.012329>.
- [3] F. W. Strauch, Phys. Rev. Lett. **109**, 210501 (2012), URL <https://link.aps.org/doi/10.1103/PhysRevLett.109.210501>.
- [4] M. Christandl, N. Datta, A. Ekert, and A. J. Landahl, Phys. Rev. Lett. **92**, 187902 (2004), URL <https://link.aps.org/doi/10.1103/PhysRevLett.92.187902>.

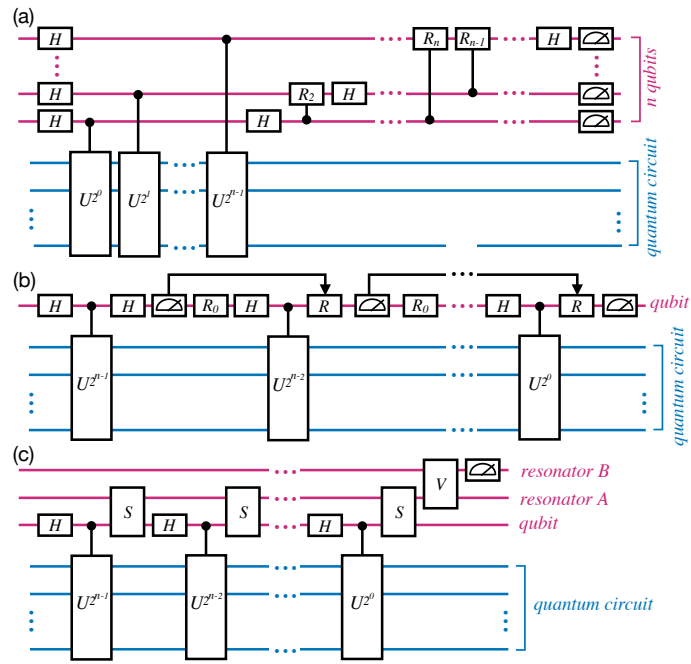


FIG. 1: Circuit diagrams for the quantum phase estimation, using (a) the conventional approach, (b) qubit recycling and (c) our approach. Here, H denotes the Hadamard gate, U^{2^k} the controlled phase gate, R_k the single or two-qubit gate. The symbol S denotes the state transfer process from a qubit to the resonator A.